

Thermo-Hydraulic Modeling of the Northern Upper Rhine Graben using OpenGeoSys

Fransiskus Litani Santoso¹, Leandra Weydt¹, Haibing Shao², Hung Pham¹ and Ingo Sass^{1,3}

¹ Department of Geothermal Science and Technology, Institute of Applied Geosciences, Technical University of Darmstadt, Germany; ² Department of Environmental Informatics, Helmholtz Centre for Environmental Research – UFZ, Leipzig, Germany; ³ Section 4.3 Geoenergy, GFZ Helmholtz Centre for Geosciences, Potsdam, Germany

Keywords: Thermo-Hydraulic Simulation, OpenGeoSys, Petrel, Upper Rhine Graben, Deep Geothermal, Hydrothermal Convection

Abstract

Effective geothermal reservoirs are characterized by high permeability, elevated geothermal gradients and active hydrothermal fluid dynamics. Targeting zones with these features is essential to ensure sufficient temperature and flow rate at the wellhead, which is the key factor for the economic viability of geothermal projects. The Upper Rhine Graben (URG) is characterized by numerous positive temperature anomalies and abundant permeable fault zones that facilitate fluid movement, which could lead to the development of hydrothermal convection cells in the subsurface. Accurately identifying such zones can substantially reduce the risk associated with geothermal prospecting. To improve the reliability of predicting the location of hydrothermal convection cells, numerical simulation can be utilized to simulate the interactions of coupled thermo-hydraulic (TH) processes in the subsurface. This study presents a workflow for integrating a 3D geological model from Petrel into OpenGeoSys (OGS) to simulate coupled TH processes in the geothermal system of the Northern URG on a regional scale. The 3D geological model is based on the ArtemIS project, which incorporates data from previous projects, including GeORG, Hessen 3D 1.0 & 2.0, and DGE-ROLLOUT. The results of the TH simulation indicate that hydrothermal convection cells develop within and around fault zones, enhancing both upward and downward fluid flow. These flow patterns lead to localized positive and negative temperature anomalies. The workflow developed in this study lays the groundwork for the ConvEx project, which aims to establish integrated exploration methods for mapping hydrothermal convection cells as key targets in deep geothermal energy exploration.

1. Introduction

In Germany, the Upper Rhine Graben (URG) is one of the most promising geothermal regions due to its high geothermal gradients and numerous fault zones that enable the transport of heat and fluids through the subsurface. The Northern URG is particularly suitable for deep geothermal energy use, as it has abundant resources and detailed geological data from previous oil and gas exploration. Previous research has shown that hydrothermal convection can cause local temperature anomalies controlled by faults (Baillieux et al., 2014; Guillou-Frottier et al., 2013), highlighting the need for accurate models and simulations to reduce exploration risks (Koltzer et al., 2019). Thermo-hydraulic (TH) simulations are important tools for understanding how heat and fluids interact underground to improve safety and support sustainable geothermal development (Kolditz et al., 2015).

This study builds on previous studies to improve understanding of hydrothermal convection in the Northern URG using 3D TH modelling with OpenGeoSys (OGS). It is based on a detailed 3D geological model created in Petrel as part of the ArtemIS project (Weydt et al., 2025), combining data from the GeORG (GeORG-Projektteam, 2013), Hessen 3D (Bär, 2012; Hintze et al., 2022; Sass et

al., 2011) and DGE-ROLLOUT (Frey et al., 2021a, b, 2022) projects. After data preparation in PyVista and mesh generation with OGSTools, a structured 3D hexahedral mesh is created to represent faults and geological layers. The TH simulations are then performed using the finite element method in OGS and visualised in ParaView. The focus is on the area around Worms, where a high density of faults is likely to favour the development of convection cells. By comparing the results with previous studies, this work contributes to refining the conceptual understanding of the geothermal system and providing a reproducible workflow for future reservoir modelling with Petrel and OGS.

2. Physical Background

The thermo-hydraulic (TH) coupling process integrates the thermal and hydraulic modules. The thermal module controls heat transport in the reservoir based on the law of conservation of energy and Fourier's law, while the hydraulic module describes the fluid flow according to the law of conservation of mass and Darcy's law. The interaction between these modules is bidirectional, with temperature changes affecting fluid properties such as density, specific heat capacity, and viscosity, whereas fluid flow controls the balance between conductive and convective heat transport (see Fig. 1). By combining conductive heat transport with fluid flow, the coupled TH process of fluid-rock interaction can be expressed mathematically as (Bilke et al., 2024):

$$(\varphi(\rho c)_f + (1 - \varphi)(\rho c)_s) \frac{\partial T}{\partial t} = \nabla \cdot (\lambda \nabla T - (\rho c)_f \mathbf{v}_D T) + S \quad (1)$$

where φ [-] is the porosity, ρ [kg m⁻³] is the density, c [J kg⁻¹ K⁻¹] is the specific heat capacity, T [K] is the temperature, t [s] is the time, λ [W m⁻¹ K⁻¹] is the thermal conductivity, \mathbf{v}_D [m s⁻¹] is the Darcy velocity, S [W m⁻³] is the radiogenic heat production, and the subscripts s and f represent the solid and fluid state. The Darcy velocity can be calculated by using the Darcy's law. It is directly proportional to the hydraulic conductivity \mathbf{K} [m s⁻¹] and the hydraulic gradient $\partial h / \partial x$ [-]:

$$\mathbf{v}_D = -\mathbf{K} \frac{\partial h}{\partial x_i} \quad \text{with} \quad \mathbf{K} = \mathbf{k} \frac{\rho_f}{\mu_f} \mathbf{g} \quad (2)$$

where \mathbf{k} [m²] is the intrinsic permeability, μ [Pa s] is the dynamic viscosity, and \mathbf{g} [m s⁻²] is the gravitational acceleration.

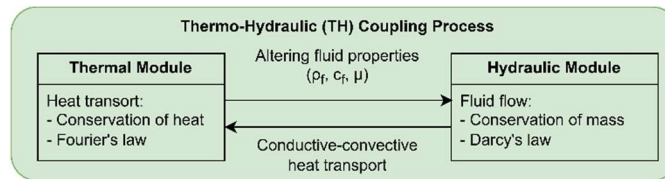


Fig. 1: TH coupling process consisting of thermal and hydraulic modules influencing each other (Santoso, 2025).

3. Geological Background

The Upper Rhine Graben (URG) is a rift valley extending NNE to SSW across southwest Germany, France (Alsace), and Switzerland (Basel), forming a 300 km long and 25-40 km wide lowland plain bordered by the Vosges, Palatinate Forest, Odenwald, and Black Forest (Frey et al., 2022). As part of the European Cenozoic Rift System, the URG formed during the Eocene due to Pyrenean and Alpine orogeny, with NE-SW to N-S compression causing crustal extension and mantle upwelling that uplifted the graben shoulders (Meschede, 2018; Ziegler, 1992). Its tectonic evolution includes three rifting phases: early uplift in the north and subsidence in the south, main subsidence during the Eocene-Oligocene, and late Neogene compression with localized uplift and subsidence (Hinsken,

2008; Schumacher, 2002). Structurally, the URG is defined by NE-SW to NNE-SSW faults inherited from Variscan structures and cross-cutting WNW-ESE faults from later tectonic events (Henk, 1993; Schwarz and Henk, 2005). Since the Miocene, activity along NW-SE normal faults has shaped its present-day geometry, producing inverted basin structures and major depositional centers such as the Heidelberg-Mannheim and Geiswasser basins (Bartz, 1974; Bossennec et al., 2022; Hagedorn, 2004).

The Upper Rhine Graben (URG) is characterized by a complex lithostratigraphic sequence that reflects its long tectono-sedimentary evolution. The geological map of the URG is presented in Fig. 2. The youngest deposits are Quaternary sediments, forming the present depocenters and supplied mainly by the Rhine River, underlain by a series of Tertiary basin fillings including the Younger Tertiary, Landau-Bruchsal, Niederroedern, Froidefontaine, and Pechelbronn formations, with the Eocene Base Clay marking the base (BGR, 2024). These unconformably overlie post-Variscan overburden rocks from the Permo-Carboniferous to the Cretaceous, which themselves rest on the Variscan crystalline basement. Regionally, the graben is largely filled with Quaternary and Tertiary sediments, though Jurassic and Triassic rocks occur in the southern part and volcanic rocks are exposed in the Kaiserstuhl. Structurally, the graben shows marked asymmetry due to multiphase rifting, with depocenters shifting between the Western and Eastern Main Boundary Faults (Bartz, 1974; Hagedorn, 2004). In the Northern URG, the Tertiary and post-Variscan units predominantly dip westward, contrasting with the structural configuration in the Central and Southern URG, which dip to the east (Frey et al., 2022).

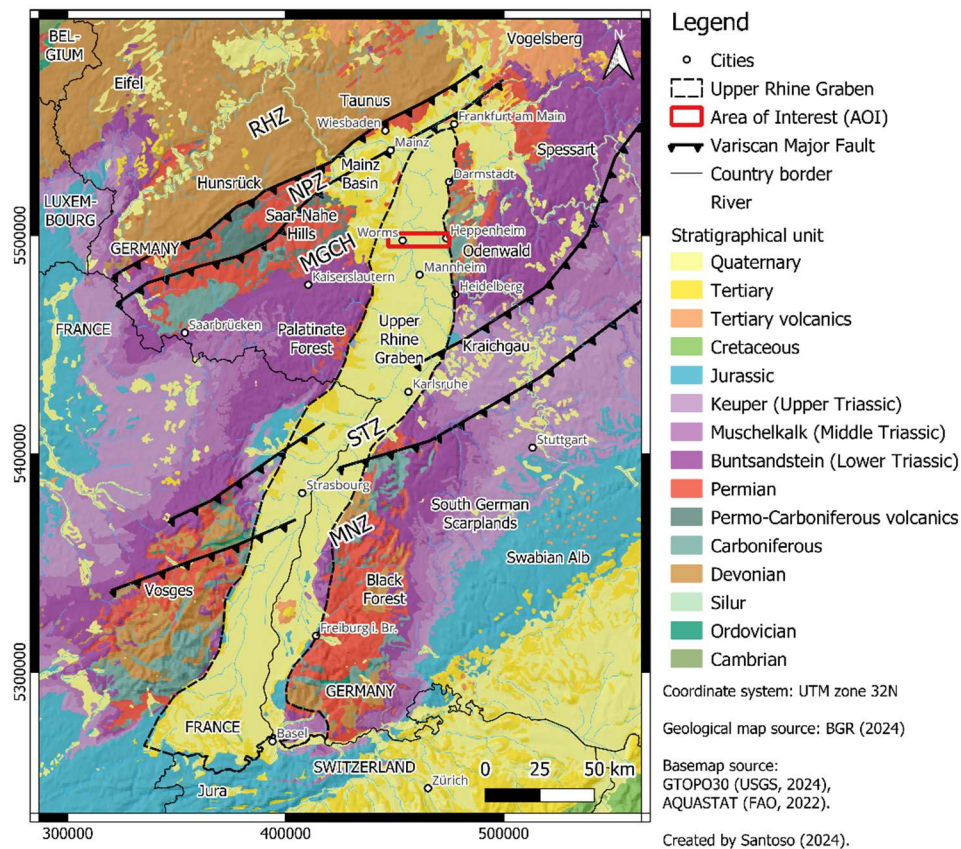


Fig. 2: Geological map of the Upper Rhine Graben with its surrounding geographical area and Variscan crystalline basement (RHZ: Rhenohercynian Zone, NPZ: Northern Phyllite Zone, MGCH: Mid-German Crystalline High, STZ: Saxothuringian Zone, MNZ: Moldanubian Zone) (Santoso, 2025). The study area is marked in red rectangle.

4. Methodology and Workflow

The 3D geological model used in this study is based on data from the ArtemIS project, which integrates results from earlier regional models such as GeORG, Hessen 3D 1.0 & 2.0, and DGE-ROLLOUT (Frey et al., 2021a; GeORG-Projektteam, 2013; Hintze et al., 2022; Perner, 2018; van der Vaart et al., 2022; Weydt et al., 2025). The input data comprise stratigraphic surface boundaries and fault geometries derived from borehole information, seismic interpretations, and other geophysical investigations. These datasets were provided in Petrel, where the 3D structural framework of the Northern URG was constructed.

For parametrization of the thermo-hydraulic (TH) simulations, thermo-petrophysical properties were assigned to each modeled geological unit of the 3D model (see Tab. 1). The required parameters include grain density (ρ_s), thermal conductivity (λ), specific heat capacity (c_s), radiogenic heat production (S), effective porosity (ϕ), and intrinsic permeability (k). These values were compiled from various previous studies and projects, notably GeORG, IMAGE, Hessen 3D 1.0 & 2.0, and AMPEDEK (Bär, 2012; Bär et al., 2020; Freymark et al., 2017; GeORG-Projektteam, 2013; Sass et al., 2011; Weinert et al., 2020; Weydt et al., 2025). Tab. 1 provides an overview of the parameter values used in the simulations.

Tab. 1: Overview of thermo-petrophysical properties of all modeled geological units for the TH simulations in OGS. Source: [1] Bär (2012), [2] Rùhaak & Sass (2013), [3] GeORG-Projektteam (2013), [4] Bär et al. (2020), [5] Freymark et al. (2017), [6] Frey et al. (2021b), [7] Bossennec et al. (2022), [8] Aretz (2016), [9] Yan et al. (2023), [10] approximated data based on simplified lithology according to VDI 4640-1 (2021). All data are mean values and refer to dry conditions.

ID	Modeled Unit	Dominant Lithology (simplified)	Effective Porosity ϕ_{eff} [%]	Intrinsic Permeability k [m ²]	Density ρ_s [kg m ⁻³]	Specific Heat Capacity c_s [J kg ⁻¹ K ⁻¹]	Thermal Conductivity λ [W m ⁻¹ K ⁻¹]	Radiogenic Heat Production S [μ W m ⁻³]
1	Young Cenozoic	Marl, sandstone, sand	17.2 [3]	$3.26 \cdot 10^{-15}$ [3]	2250 [6]	978 [10]	2.30 [3]	1.0 [5]
2	Niederroedern	Marl, limestone	18.2 [1]	$1.02 \cdot 10^{-14}$ [1]	2300 [5]	978 [10]	2.25 [3, 4]	1.0 [5]
3	Froidefontaine	Marl, limestone	13.7 [1]	$1.48 \cdot 10^{-15}$ [1]	2300 [5]	978 [10]	2.25 [3, 4]	1.0 [5]
4	Pechelbronn	Marl, limestone, dolostone	14.5 [1]	$2.82 \cdot 10^{-15}$ [1]	2300 [5]	978 [10]	2.60 [3, 4]	1.0 [5]
5	Base Tertiary	Claystone, sandstone	15.7 [3]	$2.66 \cdot 10^{-14}$ [3]	2250 [6]	1000 [10]	2.60 [3]	1.0 [5]
6	Rotliegend	Sandstones, andesite	8.9 [1, 2]	$7.24 \cdot 10^{-15}$ [1]	2430 [1]	758 [1]	2.21 [1]	1.0 [5]
7	Basement	Gneiss, granitoids	3.6 [1, 2]	$1.82 \cdot 10^{-16}$ [1]	2630 [1]	648 [1]	2.71 [1]	1.8 [5]
8	Fault Zones		25.0 [8]	$1 \cdot 10^{-13}$ [7], [8], [9]	2000 [8]	1000 [8]	2.00 [8]	1.0 [5]
9								
10								

The modeling workflow comprises five blocks (see Fig. 3). In the first block, a 3D geological model is constructed in Petrel using the structural framework workflow, and the resulting files are exported as .ts files and converted to .vtu files for use in OGS. The second block involves mesh preparation, where PyVista is applied to ensure correct fault topology, and a structured 3D hexahedral mesh is generated with ogstools.meshlib. The third block covers pre-processing steps, where 2D fault surfaces from Petrel are integrated into the 3D mesh to represent fault zones with distinct parameters, optional clipping function are developed to clip a smaller model, and both boundary and subdomain meshes are extracted for assigning boundary conditions (BCs) and source terms (STs). This step also enables cross-sectional slicing for 2D simulations if needed. The fourth block is the OGS simulation, where input data, including bulk, boundary, and subdomain meshes, are defined within a single XML-based project file (.prj), which also specifies processes, time loops, parameters, ICs, BCs, STs, and solvers. Results from steady-state heat conduction serve as initial conditions for coupled transient TH simulations. Finally, in the fifth block, post-processing is performed in ParaView, including unit conversion, visualization, contouring, glyph rendering, and data analysis.

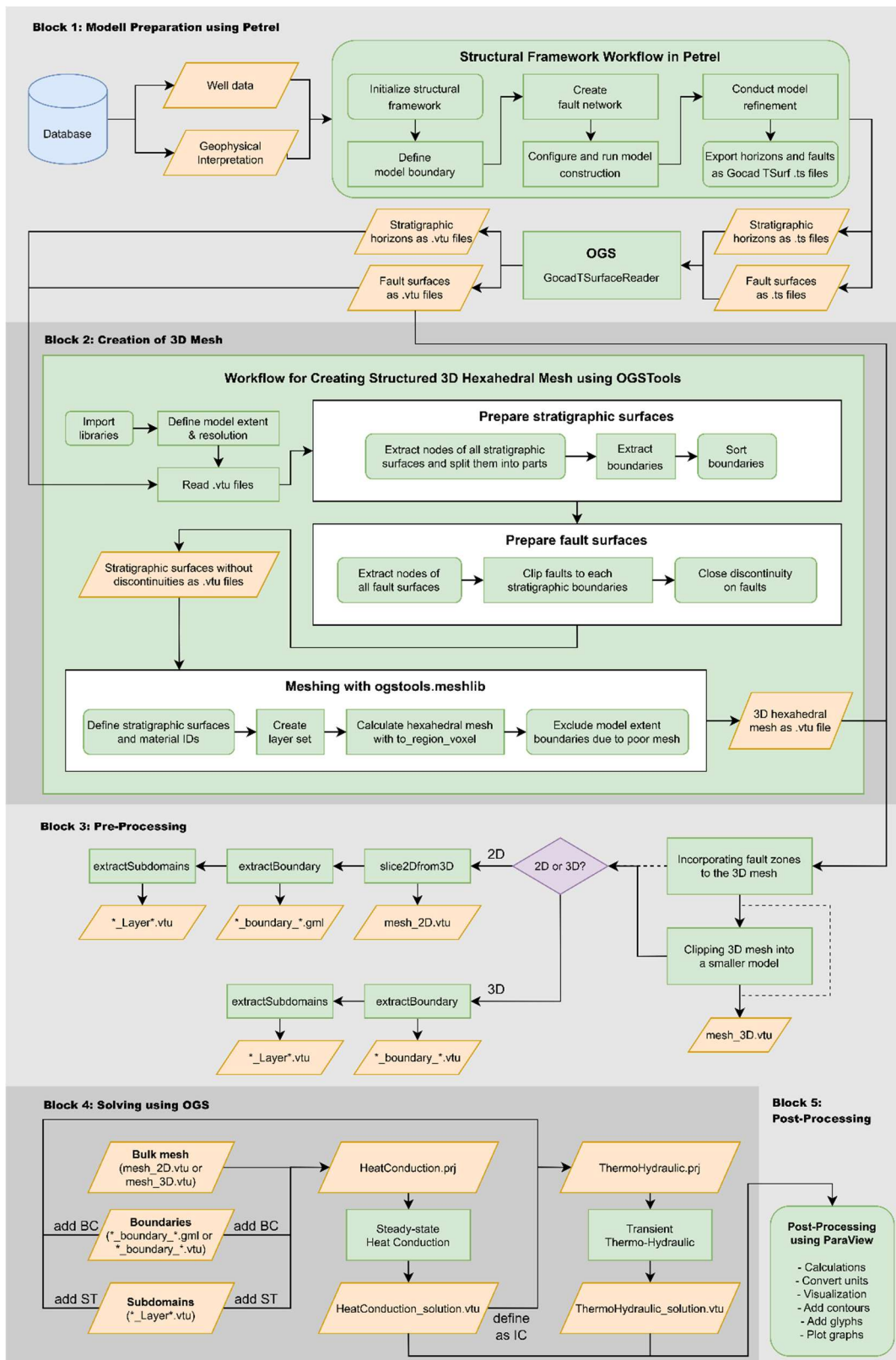


Fig. 3: Complete workflow on how to implement a 3D model from Petrel into OpenGeoSys (Santoso, 2025). BC: boundary condition, IC: initial condition, ST: source term.

5. Results and Interpretations

For the thermo-hydraulic (TH) simulations, three model domains were derived from the full 3D geological model of the Northern URG: the full model, the half-west model, and the small-west model (see Fig. 4). To make it short, only the 3D small-west model is presented in this conference publication. For details, please refer to the master's thesis by Santoso (2025). The 3D small-west model covers a western section of the graben, including the graben shoulder and the Weststrandstörung fault, with dimensions of 5.0 km (W-E), 5.7 km (N-S), and 5 km in depth.

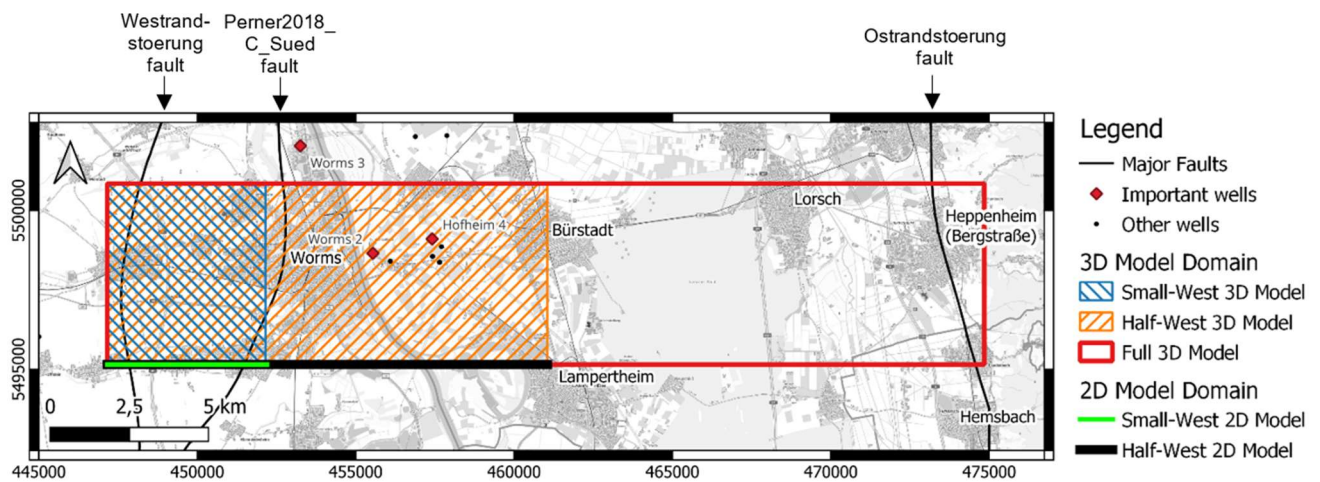


Fig. 4: Map of the model domains including major faults and wells with T-logs (Santoso, 2025). Coordinates are given in UTM zone 32N.

The 2D simulations were executed on a single-core system, whereas the 3D simulations required parallel computing on the EVE high-performance computing (HPC) cluster of UFZ. The simulations were performed on up to 32 cores using PETSc solvers, where performance tests indicated that the Conjugate Gradient (CG) method with block Jacobi preconditioning (BJACOBI) offered the best efficiency in comparison to Biconjugate Gradient Stabilized (BCGS or BiCGStab) and Generalized Minimal Residual (GMRES) methods. With this setup, a 3D simulation of a test model containing approximately 375-500k nodes required about 6-8 hours per 1,000 timesteps. These results underline the necessity of HPC resources and solver optimization for performing large-scale 3D TH simulations.

6.1 Steady-State 3D Heat Conduction Simulation

As with the 2D case (not presented in this conference publication, please refer to Santoso, 2025), the 3D simulations began with steady-state heat conduction to establish suitable initial conditions for the transient 3D TH run, with radiogenic heat production S included. The resulting temperature distribution of the 3D small-west model is ranging from about 9.5 °C at the surface to 141.5 °C at the bottom boundary at 3,745 m b.s.l.

6.2 Transient 3D TH Simulation

After 105,000 years of simulation time, the temperatures ranged from about 9.5 °C at the surface to 150.5 °C at a depth of 3,745 m b.s.l. It can be observed in the transient TH simulation that distinct thermal anomalies are developed within the model domain (see Fig. 5 left). Temperatures decreased in the southern part of the Weststrandstörung fault zone, while they increased in the northern section. This contrasting behavior reflects the influence of fluid circulation, with the northern part of the

Weststrandstörung fault zone acting as a preferential pathway for hot fluid ascent and the southern section showing cooling due to descending flows.

The flow patterns shifted significantly after 75,000 years of simulation time, when a convection cell developed within the Weststrandstörung fault zone (see Fig. 5 and Fig. 6). Fluids moved downward in the southern part of the Weststrandstörung fault zone and upward in the northern part, creating a circulation loop that explains the cooling and heating trends. The Darcy velocities vary strongly between graben zones (see Fig. 6), with the slowest flow in the basement at $0.003 - 0.2 \text{ mm a}^{-1}$, intermediate values in the Cenozoic graben inner zone at $0.1 - 27.5 \text{ mm a}^{-1}$, and the fastest flow along the fault zone at $5.0 - 179.9 \text{ mm a}^{-1}$. This distribution highlights the role of fault structures as the most efficient fluid conduits in the system.

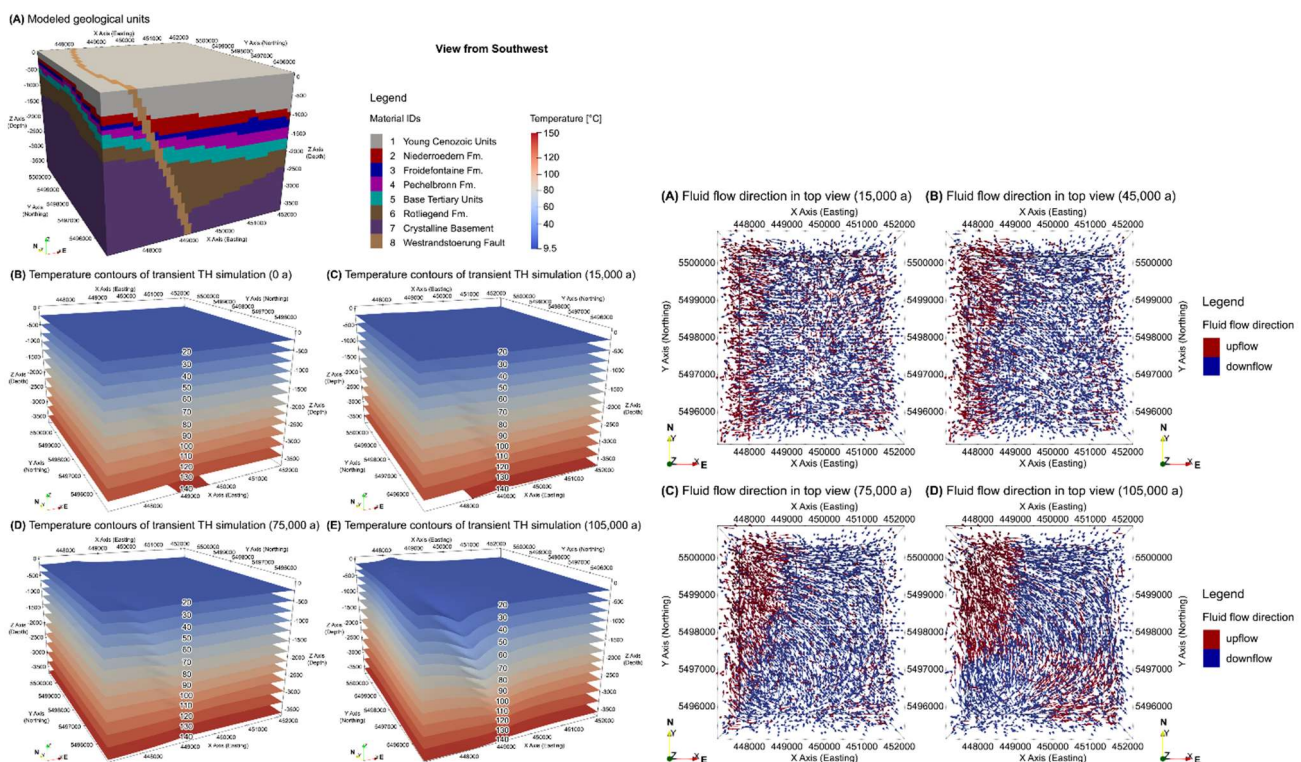


Fig. 5: Results from the transient TH simulation of the 3D small-west model. Left: Temperature contours after 0 (initial condition), 15,000, 75,000, and 105,000 years of simulation time. Right: Fluid flow direction in top view after 15,000, 45,000, 75,000 and 105,000 years of simulation time (Santoso, 2025).

6. Discussion

6.1 Model Limitation

The TH simulations in this study included several simplifications and assumptions. Several stratigraphic units were combined into a single unit, and only major faults were considered, while smaller faults were excluded. Fluid properties were simplified by using a linear temperature-dependent density and a constant viscosity. Quasi-steady-state conditions were only achieved in a few cases, reflecting the complexity and computational limitations of long-term simulations. Topography was neglected due to stair-stepping problem in structured meshes, which affected the flow and temperature patterns. Regional boundary effects and differences between 2D and 3D models further demonstrated the strong influence of dimensionality, domain size, and fault interactions on flow behavior.

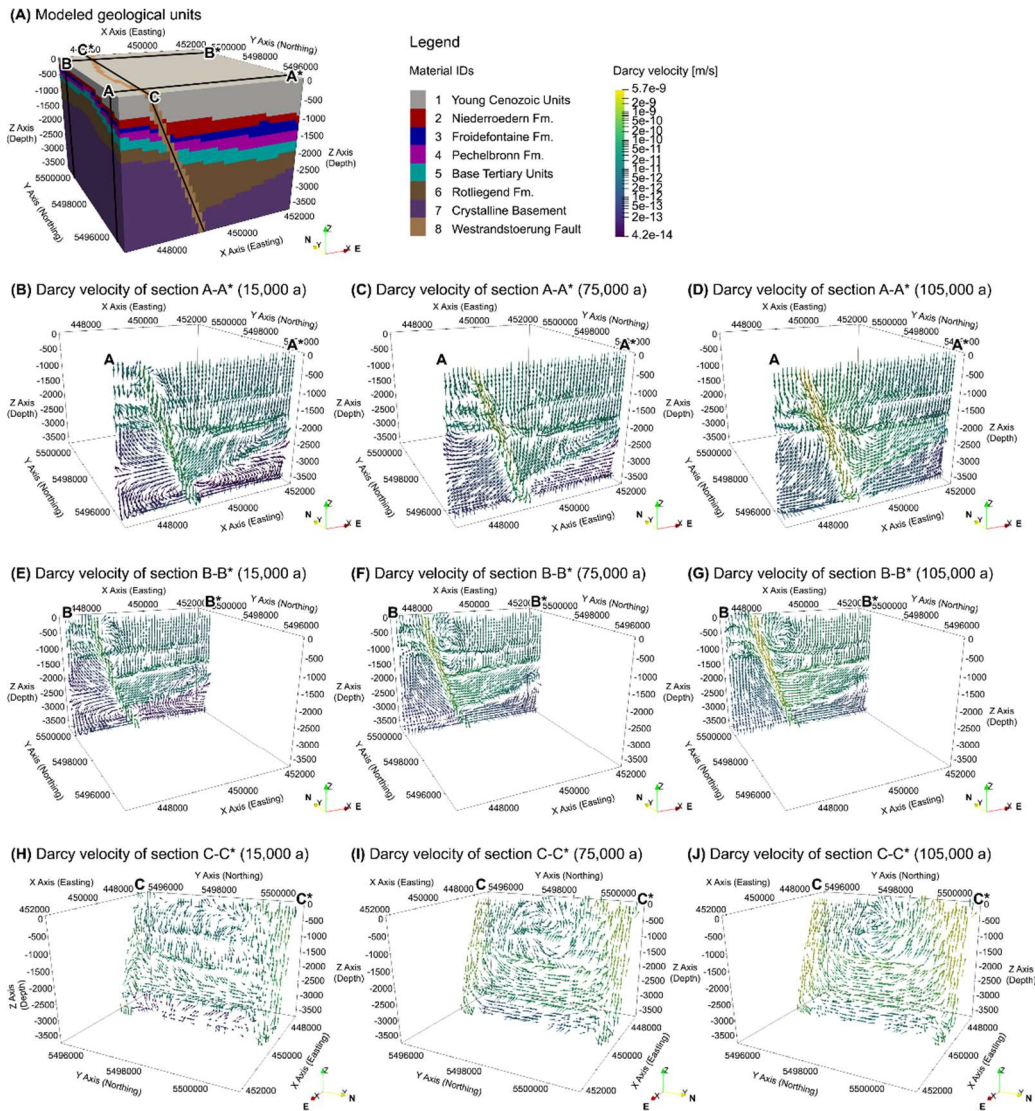


Fig. 6: Results from the transient TH simulation of the 3D small-west model. Cross sections showing Darcy velocity vectors after 15,000, 75,000, and 105,000 years of simulation time (Santoso, 2025).

6.2 Model Validation

6.2.1 Comparing modeled temperatures with previous models

As part of the Hessen 3D 2.0 project, Koltzer et al. (2019) performed a transient TH simulation of the State of Hesse using FEFLOW. Their results indicate that, at 1 km depth after 100,000 years of simulation time, temperatures in the Northern URG range from 15 °C in descending cold zones to 90 °C in ascending hot zones. A similar anomaly pattern is reproduced in the small-west model of this study using OGS, with hot anomalies in the northern part of the Westrandstörung fault zone and cold anomalies in the southern part. However, the OGS results show with 36 – 66 °C a narrower range, which may be caused by differences in modeling approaches. Koltzer et al. (2019) used constant density flow and parameterized all Cenozoic deposits as one single unit, while the TH simulation with OGS applied temperature-dependent density and subdivided the Cenozoic into five different units.

Comparison with interpolated temperatures from GeotIS (Agemar, 2022) highlights both similarities and discrepancies. At 1 km depth, OGS simulations yield temperatures of 36 – 66 °C, while GeotIS interpolation gives 56 – 70 °C, though both OGS and GeotIS show higher temperatures in the western part of the model. At greater depths, GeotIS systematically overestimates values by up to 25 °C compared to OGS. These deviations likely result from differences in resolution (2 km in GeotIS and 100 m in OGS), high standard deviations of up to ± 20 °C in GeotIS, sparse borehole data near the study area, and the fact that the OGS simulation has not yet reached quasi-steady state after 100,000 years of simulation time. All modeled and interpolated temperatures are summarized in Tab. 2.

Tab. 2: Comparing modeled temperatures with previous models.

	T [°C] 1 km b.s.l.	T [°C] 2 km b.s.l.	T [°C] 3 km b.s.l.
3D TH Simulation, OGS, Northern URG (Santoso, 2025)	36 – 66	73 – 96	115 – 126
3D TH Simulation, FEFLOW, Northern URG (Koltzer et al., 2019)	15 – 90	–	–
Interpolated Temperature, GeotIS, Northern URG (Agemar, 2022)	56 – 70	98 – 105	136 – 145

6.2.2 Comparing modeled geothermal gradients with GeotIS

The geothermal gradients from the TH simulations in OGS were compared with values from GeotIS (Agemar, 2022), which are based on well and ground-level data. In the western graben shoulder, GeotIS reports gradients of 0.040 – 0.045 K m⁻¹, while the TH simulations in OGS yield 0.034 – 0.047 K m⁻¹, showing good agreement. For the Cenozoic graben filling zone, GeotIS values of 0.030 – 0.040 K m⁻¹ are comparable to the simulated range of 0.030 – 0.042 K m⁻¹. A full overview is shown in Tab. 3.

Tab. 3: Comparing modeled geothermal gradients with GeotIS.

	$\partial T/\partial z$ [K m ⁻¹] Graben Shoulder	$\partial T/\partial z$ [K m ⁻¹] Graben Inner
3D TH Simulation, OGS, Northern URG (Santoso, 2025)	0.034 – 0.047	0.030 – 0.042
Interpolated Temperature, GeotIS, Northern URG (Agemar, 2022)	0.040 – 0.045	0.030 – 0.040

6.2.3 Comparing modeled Darcy velocities with previous models and pump tests

The Darcy velocities simulated with OGS in this study range between 0.1 and 27.5 mm a⁻¹ in the graben inner zones, which is broadly comparable to the modeled with FEFLOW by Koltzer et al. (2019) with 1 – 10 mm a⁻¹. Within the fault zones, OGS simulations yield Darcy velocities between 5.0 and 179.9 mm a⁻¹, which fall at the lower end of the fault-zone velocities obtained by Koltzer et al. (2019), who reported values between 100 and 1,000 mm a⁻¹. These differences mainly reflect variations in parameterization and differences in the study areas.

Additional comparisons confirm that the OGS results lie within the broader ranges reported in other studies. Rohrer (2015) modeled fault zones north of the study area with velocities between 2 and 9,500 mm a⁻¹, while Freymark et al. (2019) obtained a much wider spectrum of 0.49 – 5,200 mm a⁻¹ in the graben inner and 0.12 – 54,000 mm a⁻¹ in fault zones. Field-based pump tests by Aretz (2016) also support these findings, with measured Darcy velocities in fault zones ranging between 1.5 and 10,100 mm a⁻¹. Compared to these in-situ data, the OGS results show narrower ranges, likely due to model simplifications such as assuming homogeneous, isotropic porous media for fault zones, whereas natural systems are more heterogeneous and often exhibit porous-fractured characteristics. A full comparison of the Darcy velocities is provided in Tab. 4.

Tab. 4: Comparing modeled Darcy velocities with previous models and pump tests

	v_D [mm a ⁻¹] Graben Inner	v_D [mm a ⁻¹] Fault Zones
3D TH Simulation, OGS, Northern URG (Santoso, 2025)	0.1 – 27.5	5.0 – 179.9
3D TH Simulation, FEFLOW, Northern URG (Koltzer et al., 2019)	1 – 10	100 – 1,000
3D TH Simulation, FEFLOW, Northern URG (Rohrer, 2015)	–	2 – 9,500
3D TH Simulation, GOLEM, Central URG (Freymark et al., 2019)	0.49 – 5,200	0.12 – 54,000
Pump Tests, Northern URG (Aretz, 2016)	–	1.5 – 10,100

6.3 Impact of Fault Zones on Hydrothermal Convection

The TH simulations show that fault zones act as preferential pathways for fluid movement due to their high permeability, creating upflow and downflow zones that strongly influence subsurface temperature distribution. In the 2D small-west model, the Westrandstörung fault shows upward flow without topography but downward flow when topography is included, revealing the limitations of structured meshes in representing topography. The 2D half-west model further indicates that multiple faults interact, with the Westrandstörung fault channeling downward flow and the Perner-C-Süd fault facilitating upward flow, emphasizing the need to include both major and minor faults. The 3D small-west model confirms the strong influence of fault zones on hydrothermal convection dynamics, with areas of high permeability generating convection cells in which deep fluids are rapidly heated, while shallow fluids are cooled more efficiently. These patterns are crucial for geothermal exploration, as upflow zones enhance production well performance while downflow zones provide suitable locations for reinjection, supporting sustainable reservoir management.

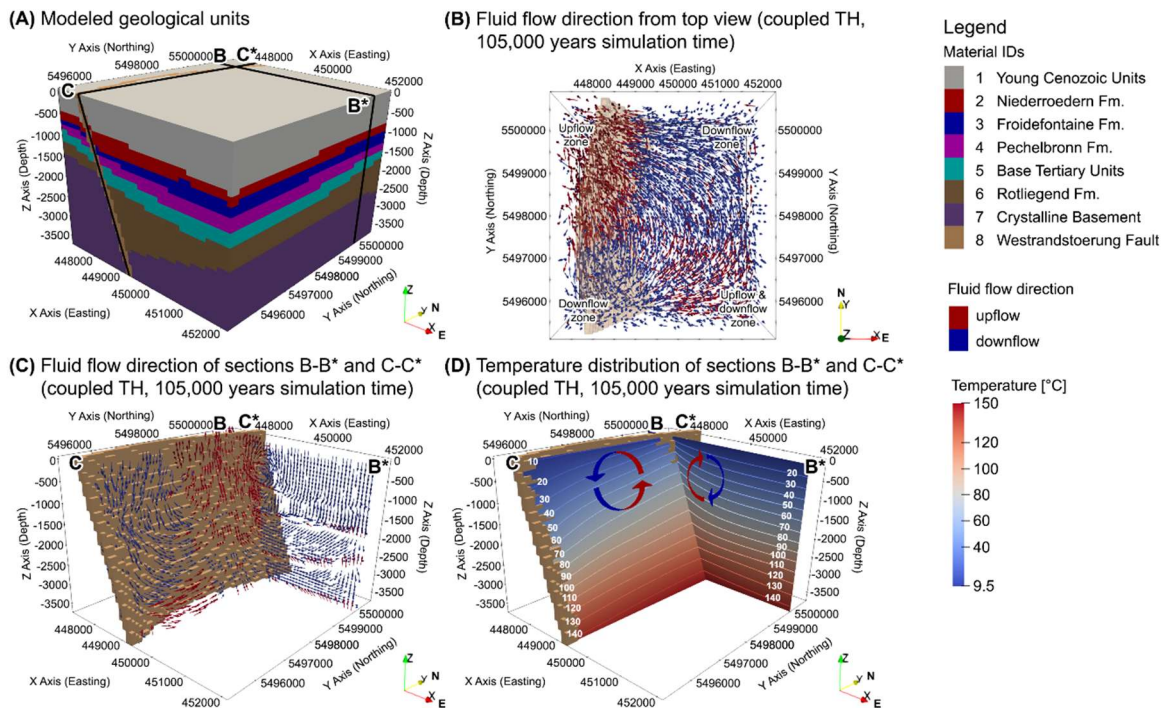


Fig. 7: Convection cells observed in the Westrandstörung fault zone after 105,000 years of simulation time. (A) Modeled geological units, (B) fluid flow direction from top view, (C) fluid flow direction in cross-sections B-B* and C-C* from southeast view, (D) temperature distribution and conceptual model of a convection cell in cross-sections B-B* and C-C* from southeast view (Santoso, 2025).

7. Conclusion and Outlook

This study successfully developed a workflow for implementing a geological 3D model from Petrel into OGS with integration of fault zones for TH simulations. The workflow consists of five main steps: (1) geological modeling in Petrel, (2) mesh generation in PyVista and OGSTools, (3) pre-processing procedures, (4) TH simulations in OGS, and (5) post-processing in ParaView. Several 2D and 3D models were clipped from the larger regional model to perform the simulations. The results highlight key limitations, including simplified stratigraphy, exclusion of minor faults, assumption of constant fluid viscosity, and neglect of topographic effects due to stair-stepping issues in structured meshes. These factors must be considered when interpreting the outcomes.

The comparison with previous studies shows that the simulated temperature and fluid flow patterns are consistent with earlier models, though differences arise from varying assumptions, boundary conditions, and modeling approaches. In general, regions of fluid upflow are associated with positive temperature anomalies, while downflow regions exhibit negative anomalies. The results also confirm the importance of fault zones, where permeability enhances both upward and downward flow. Convection cells observed in the 3D model illustrate how fault zones can act as conduits for hot fluids, creating localized temperature anomalies beneficial for geothermal exploration. Nevertheless, discrepancies with interpolated temperature data from GeotIS, particularly at depths deeper than 2 km, underline the necessity of calibrating models with borehole temperature-logs for improved reliability.

Future work should test unstructured 3D tetrahedral meshes to better capture complex topography and reduce stair-stepping effects. Since OGS does not yet support tetrahedral mesh generation with faults, external tools like Gmsh, COMSOL, or Ansys can be used. Refining mesh resolution near faults, adding smaller faults, and expanding the model domain would further improve accuracy but require more computational power. Reliable TH simulations also depend on high-quality data, including thermo-petrophysical measurements, fault zone characterization, and borehole temperature calibration. Building such datasets should be a key focus of future research.

References

- Agemar, T.: 3D Subsurface Temperature Model of Germany and Upper Austria, 2022.
- Aretz, A.: Aufschlussanalogstudie zur geothermischen Reservoircharakterisierung des Permokarbons im nördlichen Oberrheingraben, PhD Thesis, Technical University of Darmstadt, Darmstadt (2016).
- Baillieux, P., Schill, E., Abdelfettah, Y., & Dezayes, C.: Possible natural fluid pathways from gravity pseudo-tomography in the geothermal fields of Northern Alsace (Upper Rhine Graben), *Geothermal Energy*, 2, (2014).
- Bär, K.: Untersuchung der tiefengeothermischen Potenziale von Hessen, PhD Thesis, Technical University of Darmstadt, Darmstadt (2012).
- Bär, K., Reinsch, T., & Bott, J.: The PetroPhysical Property Database (P3) – a global compilation of lab-measured rock properties, *Earth Syst. Sci. Data*, 12, (2020), 2485-2515.
- Bartz, J.: Die Mächtigkeit des Quartärs im Oberrheingraben, in: *Approaches to Taphrogenesis*, Schweitzerbarth, Stuttgart (1974).
- BGR: Geologische Karte der Bundesrepublik Deutschland 1:1.000.000 (GK1000), Bundesanstalt für Geowissenschaften und Rohstoffe – BGR (2024).
- Bilke, L., Naumov, D., Wang, W., Fischer, T., Lehmann, C., Buchwald, J., Shao, H., Kizskurno, F. K., Chen, C., Silbermann, C., Radeisen, E., Zill, F., Frieder, L., Kessler, K., & Ghasabeh, M.: OpenGeoSys, (2024).
- Bossennec, C., Seib, L., Frey, M., Van Der Vaart, J., & Sass, I.: Structural Architecture and Permeability Patterns of Crystalline Reservoir Rocks in the Northern Upper Rhine Graben: Insights from Surface Analogues of the Odenwald, *Energies*, 15, (2022), 1310.
- Frey, M., Weinert, S., Bär, K., van der Vaart, J., Dezayes, C., Calcagno, P., Sass, I., & TU Darmstadt: 3D Geological Model of the Crystalline Basement in the Northern Upper Rhine Graben Region, (2021a).

- Frey, M., Weinert, S., Bär, K., Van Der Vaart, J., Dezayes, C., Calcagno, P., & Sass, I.: Integrated 3D geological modelling of the northern Upper Rhine Graben by joint inversion of gravimetry and magnetic data, *Tectonophysics*, 813, (2021b), 228927.
- Frey, M., Bär, K., Stober, I., Reinecker, J., Van Der Vaart, J., & Sass, I.: Assessment of deep geothermal research and development in the Upper Rhine Graben, *Geothermal Energy*, 10, (2022).
- Frey, M., Sippel, J., Scheck-Wenderoth, M., Bär, K., Stiller, M., Fritsche, J.-G., & Kracht, M.: The deep thermal field of the Upper Rhine Graben, *Tectonophysics*, 694, (2017), 114-129.
- Frey, M., Bott, J., Cacace, M., Ziegler, M., & Scheck-Wenderoth, M.: Influence of the Main Border Faults on the 3D Hydraulic Field of the Central Upper Rhine Graben, *Geofluids*, 2019, (2019), 1-21.
- GeORG-Projektteam: Geopotenziale des tieferen Untergrundes im Oberrheingraben, Fachlich-Technischer Abschlussbericht des Interreg-Projekts GeORG, Teile 1-4, LGRB, LGB, BRGM, AUG, Freiburg i. Br., Mainz, Strasbourg, Basel, (2013).
- Guillou-Frottier, L., Carré, C., Bourguin, B., Bouchot, V., & Genter, A.: Structure of hydrothermal convection in the Upper Rhine Graben as inferred from corrected temperature data and basin-scale numerical models, *Journal of Volcanology and Geothermal Research*, 256, (2013), 29-49.
- Hagedorn, E.-M.: Sedimentpetrographie und Lithofazies der Jungtertiären und Quartären Sedimente im Oberrheingebiet, PhD Thesis, Universität zu Köln, Köln (2004).
- Henk, A.: Subsidenz und tektonik des Saar-Nahe-Beckens (SW-Deutschland), *Geol Rundsch*, 82, (1993), 3-19.
- Hinsken, S.: Upper Rhine Graben: quantitative aspects of rifting and syn-rift sedimentation with focus on the Palaeogene series in the southern part, PhD Thesis, University of Basel, Basel (2008).
- Hintze, M., Bär, K., Bott, J., Sass, I., & TU Darmstadt: Geological-geothermal 3D model of the Cenozoic graben fill of the northern Upper Rhine Graben, Germany, (2022).
- Kolditz, O., Shao, H., Wang, W., & Bauer, S. (Eds.): Thermo-Hydro-Mechanical-Chemical Processes in Fractured Porous Media: Modelling and Benchmarking – Closed-Form Solutions, Springer International Publishing, Cham (2015).
- Koltzer, N., Scheck-Wenderoth, M., Bott, J., Cacace, M., Frick, M., Sass, I., Fritsche, J.-G., & Bär, K.: The Effects of Regional Fluid Flow on Deep Temperatures (Hesse, Germany), *Energies*, 12, (2019), 2081.
- Meschede, M.: Geologie Deutschlands, Springer Berlin Heidelberg, Berlin, Heidelberg (2018).
- Perner, M. J.: Evolution of Palaeoenvironment, Kerogen Composition and Thermal History in the Cenozoic of the Northern Upper Rhine Graben, SW-Germany, PhD Thesis, Ruprecht-Karls-Universität Heidelberg, Heidelberg (2018).
- Rohrer, L.: Fazielle und themohydraulische Modelle zur geothermischen Eignung des Permokrabons im nördlichen Oberrheingraben, PhD Thesis, Ruprecht-Karls-Universität Heidelberg, Heidelberg (2015).
- Rühaak, W., & Sass, I.: Applied Thermo-Hydro-Mechanical Coupled Modeling of Geothermal Prospection in the Northern Upper Rhine Graben, Thirty-Eighth Workshop on Geothermal Reservoir Engineering, Stanford University, Stanford, California, 2013.
- Santoso, F. L.: Thermo-Hydraulic Modeling of the Northern Upper Rhine Graben using OpenGeoSys, Master Thesis, Technical University of Darmstadt, Darmstadt (2025).
- Sass, I., Hoppe, A., Arndt, D., & Bär, K.: Forschungs- und Entwicklungsprojekt „3D-Modell der geothermischen Tiefenpotenziale von Hessen“, Technical University of Darmstadt, Darmstadt (2011).
- Schumacher, M. E.: Upper Rhine Graben: Role of preexisting structures during rift evolution, *Tectonics*, 21, (2002).
- Schwarz, M., & Henk, A.: Evolution and structure of the Upper Rhine Graben: insights from three-dimensional thermomechanical modelling, *Int J Earth Sci (Geol Rundsch)*, 94, (2005), 732-750.
- van der Vaart, J., Frey, M., Bär, K., Reinecker, J., & Sass, I.: Assessment of the Deep Geothermal Potential of Cenozoic Formations in the Northern Upper Rhine Graben using Stochastic Uncertainty Modelling, European Geothermal Congress 2022, Berlin (Germany) (2022).
- VDI: VDI 4640 Blatt 1: Thermische Nutzung des Untergrunds - Grundlagen, Genehmigungen, Umweltaspekte / Thermal use of the underground - Fundamentals, approvals, environmental aspects (2021).
- Weinert, S., Bär, K., & Sass, I.: Petrophysical Properties of the Mid-German Crystalline High: A Database for Bavarian, Hessian, Rhineland-Palatinate and Thuringian Outcrops (2020).
- Weydt, L., Agemar, T., Erb, M., Mantei, N., Dobrzinski, N., Weber, J., Sperlich, S., Van Der Vaart, J., Bär, K., Moeck, I., & Sass, I.: The ArtemIS project: Assessment for medium-depth geothermal energy utilization in Germany, *Adv. Geosci.*, 65, (2025), 199-210.
- Yan, G., Busch, B., Egert, R., Esmailpour, M., Stricker, K., & Kohl, T.: Transport mechanisms of hydrothermal convection in faulted tight sandstones, *Solid Earth*, 14, (2023), 293-310.
- Ziegler, P. A.: European Cenozoic rift system, *Tectonophysics*, 208, (1992), 91-111.

Correspondence to:
Fransiskus Litani Santoso
Institut für Angewandte Geowissenschaften
Fachgebiet Angewandte Geothermie
Gebäude B2|02 Raum 127
Schnittspahnstraße 9
D-64287 Darmstadt
santoso@geo.tu-darmstadt.de / fransiskus.santoso@gmx.de